applied sciences

MDPI

Article

Characterization of Small Micro-and Nanoparticles in Antarctic Snow by Electron Microscopy and Raman Micro-Spectroscopy

Nicolò Riboni [1,*], Erika Ribezzi [1], Lucia Nasi [2], Monica Mattarozzi [1], Maurizio Piergiovanni [1], Matteo Masino [1], Federica Bianchi [1,3,*] and Maria Careri [1]

[1] Department of Chemistry, Life Sciences and Environmental Sustainability, University of Parma, Parco Area delle Scienze 17/A, 43124 Parma, Italy
[2] CNR-IMEM Institute, 43124 Parma, Italy
[3] Center for Energy and Environment (CIDEA), University of Parma, Parco Area delle Scienze 42, 43124 Parma, Italy
* Correspondence: nicolo.riboni@unipr.it (N.R.); federica.bianchi@unipr.it (F.B.)

Abstract: The impact of the anthropic activities in Antarctica is a concerning issue. According to the Scientific Committee on Antarctic Research, attention has to be paid to the next-generation contaminants deriving from both long-range atmospheric transport and local sources. In this study, the capabilities of transmission electron microscopy with energy-dispersive X-ray spectroscopy and Raman micro-spectroscopy were exploited to evaluate the size, morphology, and chemical composition of small micro- and nanoparticles, as well as their aggregates, in surface snow samples collected during the 2020–2021 austral summer in the coastal area of Victoria Land near the Mario Zucchelli research station. The presence of biological particles, mineral dust, sea salts, and small carbonaceous and plastic micro- and nanoparticles was assessed. Sulfate, carbonate, and nitrate minerals were detected in all the samples, whereas polyethylene, poly(ethylene-co-vinyl-acetate), and different kinds of carbonaceous materials were predominantly identified in the samples closest to the research base. The presence of small micro- and nanoparticles containing heavy metals and plastic polymers in samples collected in the areas surrounding the Italian research base highlights the impact of anthropogenic activities on the polar environment, suggesting the need for continuous monitoring to evaluate possible threats to the delicate Antarctic ecosystem.

Keywords: Antarctica; small microparticles; nanoparticles; transmission electron microscopy; Raman spectroscopy

Citation: Riboni, N.; Ribezzi, E.; Nasi, L.; Mattarozzi, M.; Piergiovanni, M.; Masino, M.; Bianchi, F.; Careri, M. Characterization of Small Micro-and Nanoparticles in Antarctic Snow by Electron Microscopy and Raman Micro-Spectroscopy. *Appl. Sci.* **2024**, *14*, 1597. https://doi.org/10.3390/app14041597

Academic Editor: Elisa Sani

Received: 28 January 2024
Revised: 12 February 2024
Accepted: 13 February 2024
Published: 17 February 2024

1. Introduction

The effects of the presence of humans in Antarctica is a debated issue; although this polar region is considered relatively isolated from anthropogenic influence, it is affected by the presence of pollutants deriving from both long-range atmospheric transport (LRAT) and local sources. A variety of pollutants have been detected, including personal care products [1,2], pharmaceuticals [3], polycyclic aromatic hydrocarbons [4,5], and heavy metals [6,7], both near research bases and in wider geographical areas. Beyond direct contamination episodes, the study of the LRAT of pollutants toward polar areas is an interesting research field, since contaminants characterized by reduced environmental mobility can also be atmospherically transported over long distances [1]. Recent studies tracked the same pollutants in the treated discharges of research bases in nearby areas, according to the wind pattern, and in seawater, observing a significant increase in the concentration levels during the seasonal melt of the sea ice and of its snow cover [2].

In this context, an emerging area of research is the determination of micro- and nano-materials [8,9], including nanoparticles (NPs); quantum dots; and organic nanomaterials, such as carbon-based materials and mixed organic–inorganic nanomaterials. These substances can derive from a variety of sources, being intentionally produced or deriving from

contamination by anthropic activities [10]. In particular, due to their small size, NPs, having both organic and inorganic composition, can exert a large effect on atmospheric chemistry, together with increased environmental reactivity and toxicity. Their determination is an important issue for understanding the mechanisms of transferring pollutants through the environment. In this context, polar regions are an interesting sink for environmental contaminants; precipitation is recognized as an effective scavenger of aerodispersed matter, leading to its accumulation in the snowpack, where it can be preserved for long periods due to the low temperatures and reduced sunlight exposure [4,11].

NPs are materials with a size in the 1–100 nm range and can be either artificially engineered or produced via natural processes or human activities [12,13]. The analysis of NPs requires the use of different analytical approaches, among which electron microscopy (EM) techniques, including transmission electron microscopy (TEM) [14,15], environmental scanning electron microscopy (ESEM) [16,17], scanning probe microscopy, and atomic force microscopy (AFM) [18,19], are particularly suitable for the imaging and characterization of individual NPs due to their intrinsic sub-nanometer-scale resolution. These techniques represent a valuable tool for nanomaterial characterization in terms of morphology, size, and structure. In addition, TEM equipped with energy-dispersive X-ray spectroscopy (EDX) provides qualitative and/or semi-quantitative elemental composition information of the investigated particles using 2D chemical spatial mapping, also at the nanoscale level. These unique features are crucial for effective particle classification. Moreover, unlike bulk methods, TEM/EDX can also reveal the mixing state of particles, showing the coexistence of different chemical and physical phases within a particle. This significantly contributes to a comprehensive understanding of their sources and their impacts on the environment [20]. When applied to the study of carbonaceous particles, TEM enables a focused examination that characterizes and discriminates between various particle types, including nanoplastics, black carbon, and organic matter [21]. This advanced analysis provides valuable insights into the probable sources of emission, allowing for differentiation between natural and anthropogenic origins.

Concerning the determination of micro- or nanoparticles, additional techniques based on thermal analytical methods coupled with mass spectrometry [22,23] or vibrational spectroscopy, including Fourier transform infrared spectroscopy (FTIR) and Raman spectroscopy [24–28], can be applied to determine information about the sample composition. Whereas pyrolysis–gas chromatography coupled with mass spectrometry has proven to be effective for nanomaterial analysis [11,29], both FTIR and Raman micro-spectroscopy are non-destructive techniques suitable for the detection of sub-micromaterials, providing detection limits of about 20 μm and 1 μm [30,31], respectively. Raman micro-spectroscopy is frequently used as a valid alternative to infrared spectroscopy due to its common advantages of high efficiency, negligible interference from water, and intrinsically higher spatial resolution.

In addition, liquid chromatography–mass spectrometry (LC-MS) is expected to evolve as one of the most versatile and reliable analytical techniques for the characterization of NPs, offering a valuable tool to advance the knowledge of the properties and behavior of nanomaterials and to monitor their eventual long-term effects on health and the environment, which have not been predicted so far [32]. With reference to micro- and nanoplastics, the LC-MS technique plays an important part in the context of their pollution, since it can be used not only for particle detection, identification, and quantification but also for the determination of organic contaminants in micro- and nanoplastic samples by studying sorption/migration phenomena [33].

In the context of a research project that aimed to develop innovative analytical methods to characterize the chemical load present in polar regions, with a focus on micro- and nanoparticle contamination in Antarctic snow, in this study, TEM/EDX and Raman micro-spectroscopy were exploited to qualitatively evaluate critical parameters such as the size, morphology, and chemical composition of individual particles and their aggregates at the micro/nanoscale. This information can be of pivotal importance to assess the occurrence

and distribution of small micro- and nanomaterials in remote regions, identifying potential sources, and their impact on the environment.

2. Materials and Methods

2.1. Sample Collection

Surface snow samples were collected in the coastal area of Victoria Land (Antarctica) near Mario Zucchelli Station, one of the Italian research bases in Antarctica, located in Terra Nova Bay, along the coast of the Northern Foothills, north-east of Gerlache Inlet. The sampling coordinates are reported as follows: sample A was collected from the Icaro Camp meteorological station area (74°42′37″ S, 164°07′05″ E), sample B near Enigma Lake (74°42′38″ S, 164°01′10″ E), sample C from Browning Pass (74°36′55″ S, 163°56′29″ E), sample D near Cape Phillips (73°03′41″ S, 169°36′16″ E), and sample E from Adelie Cove (74° 45′ 40″ S 169° 36′ 16″ E) (Figure 1). All the samples were obtained during the 2020–2021 austral summer and kindly provided by the National Antarctic Research Program (PNRA) "Emerging COntaminants in Antarctic Snow: sources and TRAnsport ECO:ASTRA". Environmental variables related to the sampling campaign have been reported in previous studies [34,35]. Snow samples were manually sampled after the removal of the uppermost superficial layer (0.3–0.8 cm) using pre-cleaned premium-grade polystyrene accuvettes to prevent contamination, with a maximum depth of 12 cm [6]. The samples were collected using both wide-mouthed glass and acid-pre-cleaned HDPE bottles (500 mL volume). All the glass bottles were rinsed twice with deionized water and dried prior to sampling. The operators wore clean-room clothes and approached the sampling areas upwind from the dominant wind direction. To prevent sample contamination, motorized activity was interrupted about 300 m from the collecting site. All the samples were frozen immediately after collection and maintained at −20 °C until analysis.

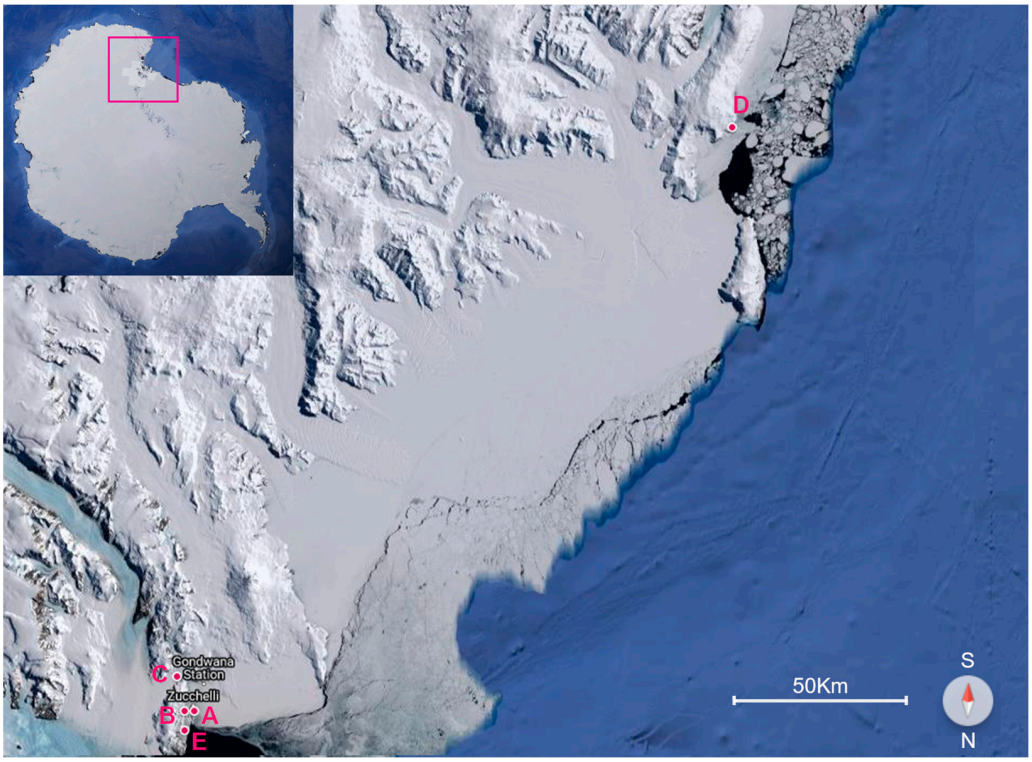

Figure 1. Sampling sites (A–E) of surface snow in Antarctica.

All the glassware and materials used for sampling, filtering, or analysis were thoroughly cleaned following the procedure proposed by Grotti et al. [6], which required consecutive cleaning steps using 10% *v*/*v* analytical-grade nitric acid (nitric acid 65% Merk,

Milan, Italy), 1% v/v suprapure-grade nitric acid (suprapure nitric acid 65%, Supelco, Bellefonte, PA, USA), and ultrapure water (Milli-Q water).

2.2. TEM/EDX Analysis

After melting the samples at room temperature, a preliminary size-separation step was carried out by filtering the melted snow by using 25 mm polycarbonate cyclopore membranes (Whatman Inc., Chalfont St. Giles, UK) with a pore size of 2 µm, followed by a subsequent filtering step using 0.40 µm filters and the collection of the filtrate into an acid (HNO_3)-pre-cleaned beaker to prevent contamination [7]. All the steps were carried out in a clean room, and the operators wore cotton clothes. After filtration, a 150 mL aliquot was reduced to approximately 500 µL through gentle evaporation to prevent potential nanoparticle loss [6]. Fifteen drops, each with a volume of 10 µL, were drop-cast onto ultrathin holey carbon films supported by a copper TEM grid (Ultral-Thin Carbon Film Supported Copper Gilder Finder F1 Grids, Merk, Milan, Italy), allowing the partial drying of the grid after each individual drop.

TEM analyses were performed with a JEOL JEM-2200FS microscope (Milan, Italy) operating at 200 kV, equipped with an Oxford detector (80 mm^2) (Oxford Instrument, High Wycombe, UK) for imaging and EDX spectroscopy. The images of individual particles were taken in both conventional TEM imaging mode and high-angle annular dark-field scanning TEM mode (HAADF-STEM). To ensure the representativeness of the analyzed particles, 10 mesh areas of the grid, each covering an area of approximately 10^4 μm^2, were examined, encompassing particles from both the center and periphery. Field blank analyses were conducted to identify and exclude potential contamination during the entire sampling, storage, and preparation process. One hundred and fifty milliliters of Milli-Q water was analyzed in accordance with the same procedure described above.

2.3. Raman Micro-Spectroscopy

The snow samples stored in glass bottles were melted at room temperature and filtered using 25 mm SPI-pore polycarbonate membrane filters with a pore size of 20 µm (SPI Supplies, West Chester, PA, USA). While operating in a clean room, the filtrate was collected into a pre-cleaned beaker to avoid contamination. Five drops of the sample were deposited on an aluminum-covered slide and subjected to Raman analysis. Raman spectra were acquired with a Horiba LabRAM HR Evolution Raman micro-spectrometer (Horiba, Kyoto, Japan) equipped with a liquid-nitrogen-cooled CCD. A 633 nm He-Ne laser coupled with a ULF Bragg filter was used for excitation, and the laser power was adjusted to below 1 mW to avoid the thermal decomposition of the samples. Daily calibration was performed with a silicon slice using the 520.6 cm^{-1} band.

Field blank analyses were conducted to identify and exclude potential contamination during the entire sampling, storage, and preparation process. One hundred and fifty milliliters of Milli-Q water was analyzed in accordance with the same procedure described above.

The investigated region was approximately 500 µm × 500 µm. The region of interest was first optically imaged with 10× magnification in order to identify and locate micro- and sub-microparticles, and then the Raman spectrum of each particle was collected with a 100× magnification objective. Due to the presence of different particles, ranging from microplastic materials to carbon soot and inorganic particles, the acquisition parameters were modified to ensure the best signal-to-noise ratio, always starting from the minimal laser power (below 0.1 mW) to protect materials from thermal degradation. The exposure time was fixed from 10 to 30 s, with 3 to 6 spectral accumulations. The LabSpec Spectroscopy Suite (version 6.4.1.51) software was used for data analysis. Compound identification was carried out by comparing the acquired spectra with those stored in the PublicSpectra open Raman spectral database [https://publicspectra.com/, last access 9 January 2024] and rruff database (https://rruff-2.geo.arizona.edu/, last access 9 January 2024).

3. Results

The processes involved in the transport and deposition of pollutants in polar regions are complex and still require additional investigations. Although heavy metals or persistent organic pollutants [5,6] have been used as proxies of environmental change, nowadays, emerging contaminants represent an additional issue of concern [2,10]. In Antarctica, it has already been observed that contamination can derive from both local sources and long-range transport. Previous studies highlighted the presence of metals, namely, Cd, Cr, Cu, Pb, and Zn, in particulate matter [7,36] and microplastics [37] related to the activities of the research stations in Antarctica, with wastewater, heating systems, and outdoor clothing or equipment being the major sources of contamination [7,37,38]. However, additional inputs derive from long-range transport. In this study, five samples of Antarctic snow collected in Terra Nova Bay were analyzed to investigate the presence of small micro- and nanomaterials, exploiting the capabilities of both TEM/EDX and Raman microspectroscopy. In particular, four samples were collected in areas neighboring the Italian research station Mario Zucchelli, located in the Ross Sea area in Victoria Land, and one sample in Cape Phillips, 250 km NE from the station.

3.1. TEM/EDX Analysis

The deposition method resulted in a surface density of approximately 10^4 nanoparticles per square millimeter. The particle size distribution at the nanoscale is illustrated in Figure 2: no significant variation was observed across the collected samples.

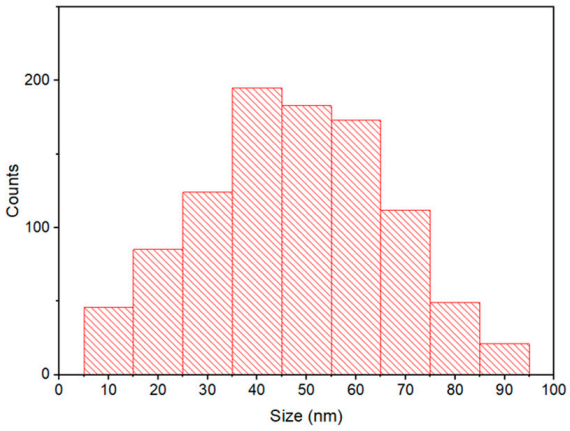

Figure 2. The size distribution of the nanoparticles in the snow samples.

Particles of different origins were observed: based on their composition and morphology, the particles were classified as biological, mineral dust, S-rich, sea salt, carbonaceous, and metal oxide nanoparticles, with mineral dust being the most abundant class, followed by carbonaceous nanoparticles. Table 1 summarizes the types of particles, including their structural/morphological properties, size, and sampling locations. Representative TEM images of these categories are illustrated in Figure 3.

Diatoms and marine salts were predominantly identified in the samples collected near the coast (sample D), indicating a significant influence of marine aerosols on the composition of the snow. Additionally, S-rich particles were abundant in the sample closest to the coast, and their origin could be attributed to marine phytoplankton, as reported in a previous study [28]. As represented by the HAADF image and EDX maps (Figure 4), numerous mineral dust particles and aggregates, characterized by irregular shapes and sharp edges, were identified in all samples. These particles were mainly constituted by O, Na, Si, Al, Ca, P, K, Mg, and Fe, and their origins were attributed to natural geological processes, meaning they originated from the Earth's crustal surface and were further dispersed through LRAT [6,7].

Table 1. Type and morphology of particles detected in each sample.

Particle Types	Major Elements	Structure and Morphology	Size	Samples
Biological	O, SI, Al	Amorphous, mainly diatoms	>500 nm	D
Mineral dust	O, Na, Si, Al, Ca, P, K, Mg, Fe	Crystalline and amorphous, irregular shapes with sharp edges	>10 nm	All samples
S-rich	Mainly S, minor Cl, Si	Amorphous, sponge-like morphology	50–150 nm	All samples, abundant in D
Sea salt	Na, Cl, S, Mg	Crystalline, mainly cubic	>200 nm	D
Soot	Mainly C and O and traces of S, Ca, K, Pb, Zn	Chain-like aggregates of nearly spherical carbon nanoparticles; onion-like nanostructure of graphitic layers	10–100 nm	A, B
Fly ash	Mainly C, Si, Al, and Fe and contributions from P, Mg, Ca, and K	Amorphous, spherical shape	50–300 nm	A, B, C, E
Mixing state of individual particles	C, O, Na, Si, Al, Ca, P, K, Mg, Fe	Crystalline and amorphous, aggregates of fly ash, soot, and mineral dust. Core-shell and complex morphology	>100 nm	A, B, C, E
Ti/Fe oxide nanoparticles	Ti, Fe, O	Crystalline, isolated or aggregated	5–100 nm	A, B, C, E
Cd oxide nanoparticles	Cd, O	Crystalline, isolated	50–100 nm	A, B

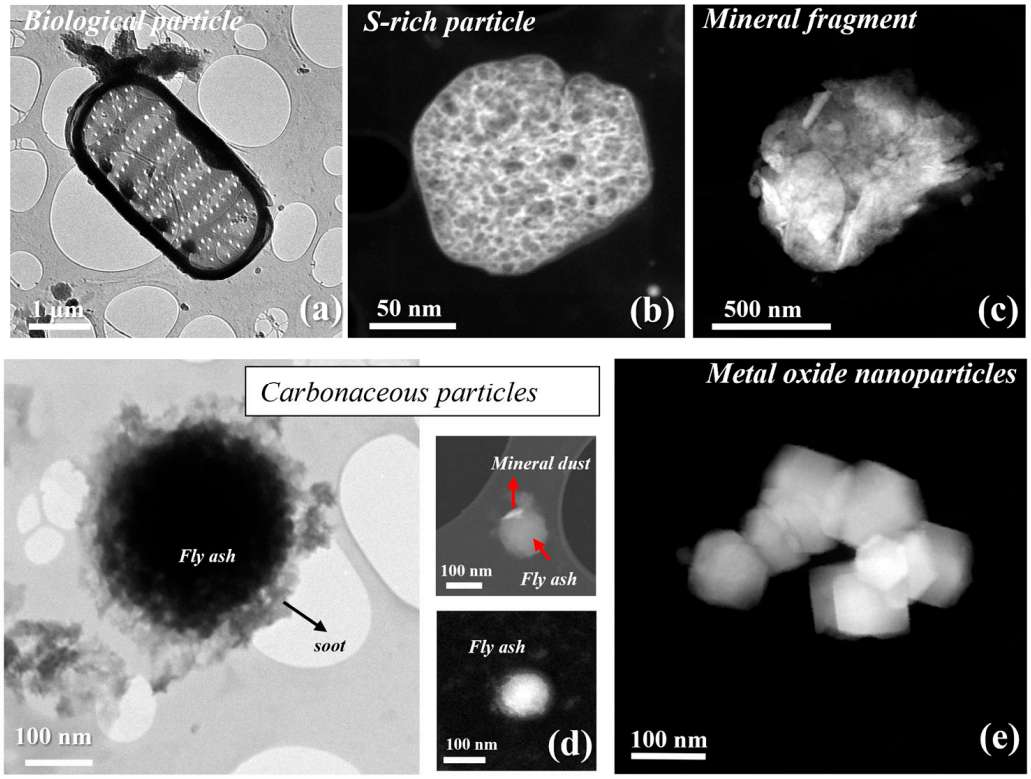

Figure 3. TEM images showing the typical and more abundant particles in the snow samples. (**a**) A TEM image of a diatom; (**b**) a HAADF-STEM image of a S-rich particle; (**c**) a HAADF-STEM image of a mineral fragment; (**d**) TEM and HAADF-STEM images of different mixed carbonaceous nanoparticles; (**e**) a HAADF-STEM image of metal oxide nanoparticles.

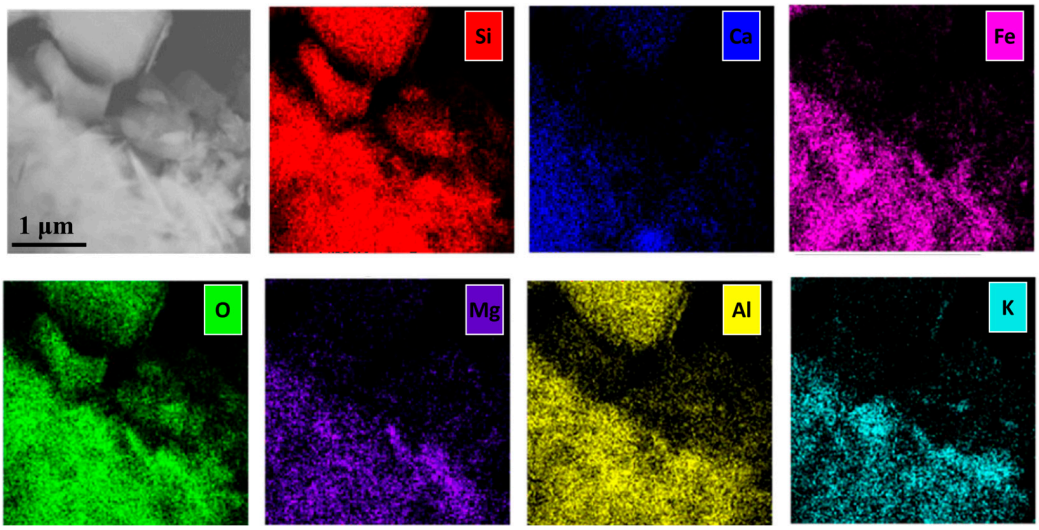

Figure 4. A HAADF-STEM image and the corresponding EDX maps of a mineral dust particle detected in sample A.

The presence of soot and fly ash particles in the Antarctic snow can be attributed to both local sources and LTRA. Locally, contributions arise from the research stations and anthropogenic activities involving the combustion of fossil fuels for transportation (ships, vehicles, aircraft) and power generation, as well as for heating. On the other hand, long-distance sources encompass natural events such as wildfires, volcanic eruptions, and specific natural processes characterized by the incomplete combustion of organic matter. Various carbonaceous particles, ranging from a few nanometers to a few hundred nanometers, were predominantly identified in the samples closest to Mario Zucchelli Station (samples A and B). The primary type of these carbonaceous particles consisted of soot characterized by quasi-spherical carbon nanoparticles with typical diameters ranging from 10 to 100 nm: these particles aggregated into chain-like structures extending up to one micron, probably due to aggregation phenomena occurred during the evaporation step (Figure 5a,b). Some soot nanoparticles displayed an onion-like nanostructure of graphitic layers when observed at high resolution (Figure 5c). They were predominantly composed of C and O, although traces of S, Ca, and K were observed in some soot particles. Notably, one soot aggregate showed traces of Pb (Figure 5d). Soot was also observed decorating fly ash particles and mineral dust, forming large mixed aggregates and core–shell structures, as reported in Figure 3d.

In addition to soot, various amorphous spheroidal carbonaceous particles, ranging from 50 to 300 nm, were identified: the most common elements included Si, Al, Fe, with additional contributions from P, Mg, Ca, and K. Based on their morphology and composition, these particles could be attributed to fly ash particles. Fly ash particles were often adorned by mineral dust and soot particles. This unique characteristic imparted complexity to their morphology, with particles having spherical shapes with round or sharp edges and sometimes exhibiting core–shell structures (Figure 3d).

A high concentration of iron and titanium oxide nanoparticles, having dimensions lower than 100 nm, in either isolated or aggregated forms, was observed in all analyzed samples except for sample D, located 250 km NE from the Italian research station. These findings could be related to increased levels of contamination deriving from the presence of the research base. An aggregate containing both types of nanoparticles is presented in Figure 6a. Moreover, EDX analysis revealed the presence of Zn and heavy metals, including Cd and Pb, predominately in the samples collected near Mario Zucchelli Station (A, B, C, E). In particular, Cd was identified in the form of cadmium oxide nanoparticles (Figure 6b), whereas Pb was localized in the proximity of soot particles. The identification of these elements in Antarctic snow samples was not surprising: as reported in previous

studies [6,36], snow samples collected near the Ingrid Christensen Coast of East Antarctica and Dome Concordia were characterized by the presence of several trace elements, such as Zn, Cu, Mo, Cd, As, Se, Sb, and Pb. These elements were very abundant compared with known natural sources, thus suggesting their anthropogenic origin.

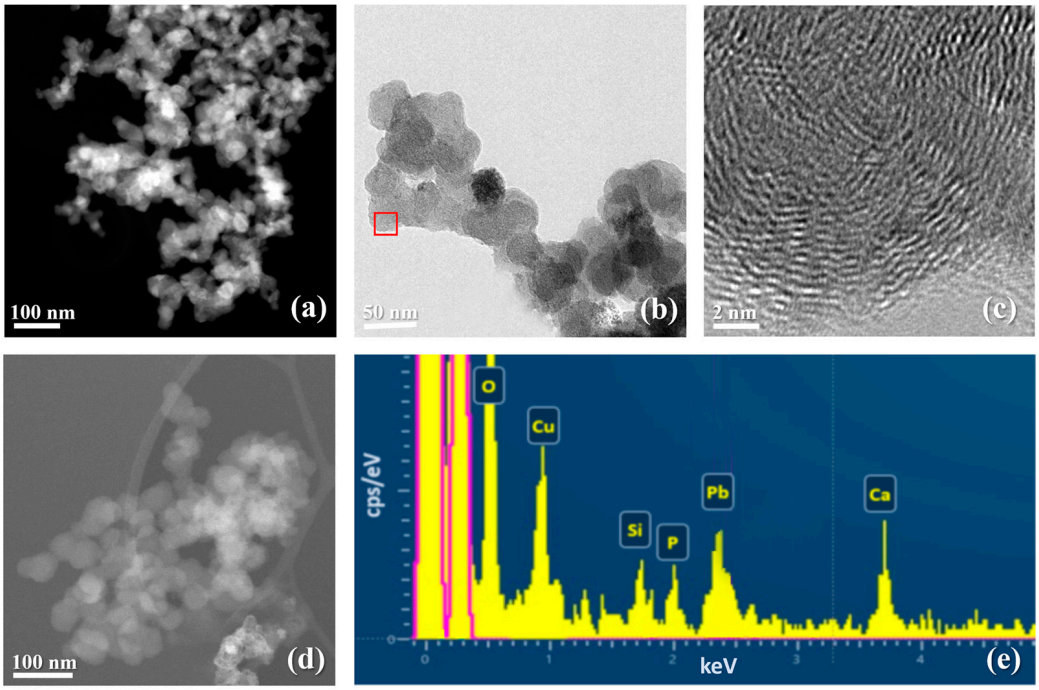

Figure 5. TEM/EDX analysis of soot observed in the samples closest to Mario Zucchelli Station. (**a**,**b**) HAADF-STEM and TEM images of chain-like clusters of soot nanoparticles, respectively; (**c**) a high-resolution TEM image of the red-line-boxed area in (**b**); (**d**) HAADF-STEM/EDX analysis of soot aggregate containing Pb; (**e**) EDX spectrum of soot aggregate.

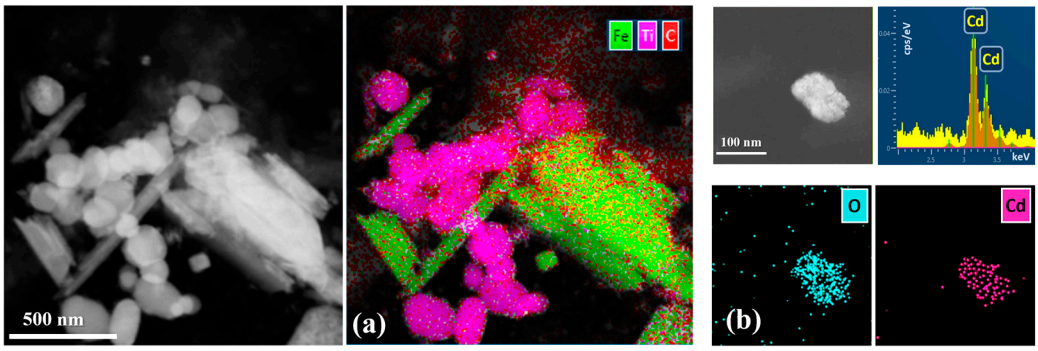

Figure 6. A HAADF-STEM image with the corresponding EDX maps of metal oxide nanoparticles observed in sample A containing (**a**) Fe and Ti; (**b**) Cd. In the EDX spectrum, the L-lines profile of Cd (brown) is superimposed on the collected spectrum (yellow).

3.2. Raman Micro-Spectroscopy

Raman micro-spectroscopy was applied in this study for the characterization of small micromaterials (1–20 μm). The use of a 633 nm laser allowed for obtaining good-quality spectra: in only some cases, the 785 nm laser source was more effective in reducing the fluorescence background. The majority of microparticles identified in the melted snow samples were minerals, carbonaceous particles, and small microplastics.

According to the results obtained by TEM analyses of NPs, in all the samples located near the research base (A, B, C, E), small microparticles of carbonaceous origin were

identified. As reported in Figure 6, the Raman spectra of these particles showed the presence of two characteristic broad overlapping bands at 1585 cm^{-1} and 1360 cm^{-1}, corresponding to the so-called G and D bands, respectively. The identification of such carbonaceous particles is still a debated issue, since different shapes and intensities of the bands could be related to the nature of carbon. It is known that the G peak is associated with the E2g mode of bulk crystalline graphite, whereas the D peak appears when the graphite breaks down near the crystal edges. Finally, the presence of both peaks suggests that the particles were formed by amorphous carbon, i.e., a combination of crystalline graphite and non-graphite elements [39]. The Raman response of the carbon particles was not different for most of the analyzed samples, with the intensity of the D band being higher than that of the G band (Figure 7a,b). Some exceptions were found in sample A, where a few particles were characterized by an inversion of the band intensities (Figure 7c). As stated in previous studies [40,41], these findings could suggest the existence of different sources of carbonaceous particles.

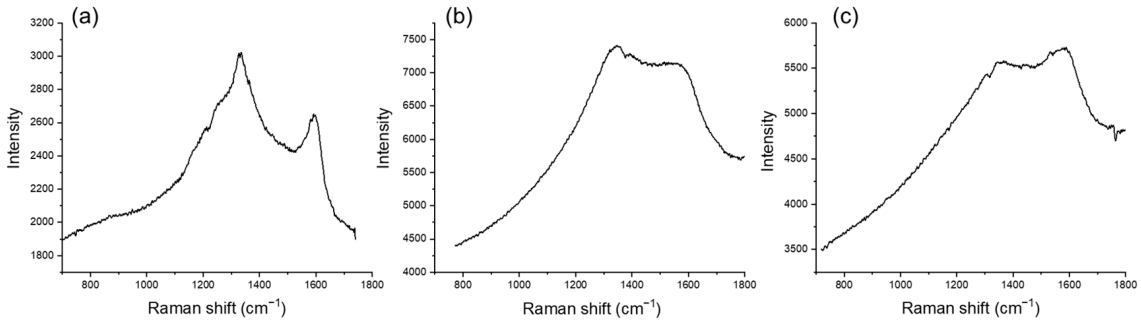

Figure 7. Raman spectra of different small carbonaceous microparticles present in sample A: (**a**,**b**) carbon particles characterized by the D band being higher than the G band; (**c**) a particle with inverted band intensities.

Minerals, including sulfates, carbonates, and nitrates, were present as the most abundant species in all the samples. Figure 6 shows some examples related to burkeite—$Na_6(CO_3)(SO_4)_2$ (RRUFF ID spectra R060112) (Figure 8a) [42,43]; sodium nitrate—$NaNO_3$ (Figure 8b) [28]; and glauberite—$Na_2Ca(SO_4)_2$ (RRUFF ID R050350) (Figure 8c) [43,44].

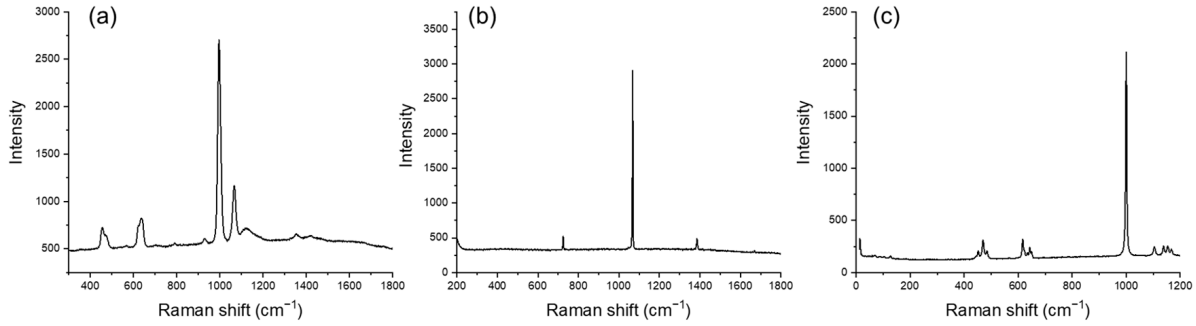

Figure 8. Raman spectra of (**a**) burkeite, (**b**) sodium nitrate, and (**c**) glauberite.

Many inorganic species have already been identified in previous studies. As in the case of carbonaceous particles, their origins are still debated. In particular, a study dealing with the characterization of Antarctic aerosol samples collected during austral summer and winter revealed the increased presence of nitrates and sulfates in the samples collected during summer as a consequence of high phytoplankton activity [28]. In a different study, the origin of sulfate in Antarctic dry-valley soils was ascribed not only to wind-blown sea salt but also to the atmospheric oxidation of reduced gaseous sulfur compounds [45].

Small microplastics were the other class of identified particles. In this study, attention was paid to particles < 20 μm. They were identified in all samples with diameters in

the 2–20 µm range, but differences in their composition were observed. More precisely, polyethylene (PE) particles were common to all the sampling sites. This polymer has been frequently detected in Antarctica: Cincinelli and coworkers [27] detected polyethylene (PE) and polypropylene (PP) as the dominant polymers in surface waters near shore and off-shore the coastal areas of the Ross Sea. PE, PP, and polyethylene terephthalate were also detected in polar ice by different research groups [11,46].

In this study, poly(ethylene-co-vinyl-acetate) (PEVA) particles having dimensions in the 15(±10) × 12(±6) µm range were also observed in samples A, B, and C. An example of the Raman spectrum of PEVA is reported in Figure 9 with the characteristic bands of the polyethylene structure due to C–H stretching frequencies (around 3000 cm^{-1}), C–H bending and twisting (1296 and 1440 cm^{-1}), and C–C stretching (1063 and 1130 cm^{-1}), along with the band at 1730 cm^{-1} marking the C=O carbonyl group of the acetate.

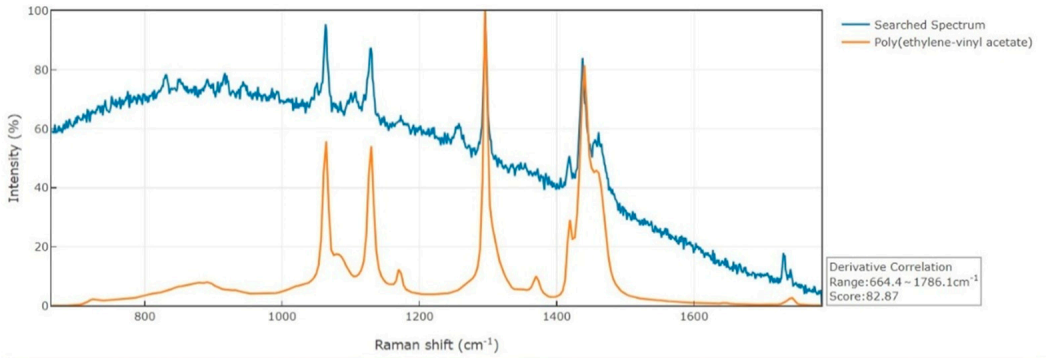

Figure 9. The Raman spectra of PEVA: the experimental spectrum (blue) vs. the spectrum stored in the PublicSpectra open Raman spectral database (yellow).

PEVA is a copolymer of vinyl acetate and ethene monomers with excellent mechanical properties and resistance to ozone, weather, and UV. It is a low-cost material used for a large variety of applications, including the use as an encapsulant for photovoltaic modules or daily-use products [47]. Therefore, the presence of this copolymer in the samples collected near the Italian research base could be ascribed to the predominant effect of a local pollution source due to anthropogenic activities, such as the recent installation of a photovoltaic plant at Mario Zucchelli Station.

3.3. Occurrence of Small Micro- and Nanoparticles in Antarctica

Our findings demonstrated the presence of small microplastics and nanoparticles related to anthropic activities, mostly detected in the area facing Terra Nova Bay, where four scientific research stations are active, namely, Mario Zucchelli Station (74°41′45″ S, 164°6′20″ E), Jang Bogo Station (74°37′27″ S, 164°13′32″ E), Gondwana Station (74°38′7″ S, 164°13′18″ E), and Qinling Station (74°52′15″ S, 163°39′50″ E). By contrast, only nanoparticles composed of elements typical of the crustal surface were detected in Cape Phillips, located about 250 km NE from the previously mentioned research stations. Unfortunately, due to the reduced number of samples, no distribution studies or comparative analyses considering different sampling periods could be performed. Nevertheless, this study adds valuable knowledge to the field of environmental contamination and its potential sources in Antarctica, a region with unique ecological significance.

Previous studies highlighted the presence of major crustal components and trace metals having an anthropogenic origin in Antarctica. Grotti et al. analyzed dissolved and particulate phases in samples from Terra Nova Bay, Talos Dome, and Dome Concordia [6,7], highlighting higher enrichment factors of anthropogenic elements, namely, Cd, Cr, Cu, Pb, and Zn. Bazzano et al. analyzed size-segregated aerosol samples collected in different areas of Terra Nova Bay, quantifying major and trace elements, as well as the lead isotopic composition, to better understand their origin and transportation pathways [48]. The

major elements, e.g., Al, Co, Fe, and Mn, were mainly related to crustal sources, whereas the marine contribution was significant for Li, Mg, and Na. An anthropogenic impact was demonstrated for Cr, Cu, Mo, and Pb; the analysis of lead isotope ratios confirmed both natural and anthropogenic inputs, with the long-range transport of polluted aerosols from South America and Australia. Thamban et al. [36] investigated the distribution and source pathways of metals in surface snow from ice-free and ice-covered areas along a coast-to-inland transect in the Ingrid Christensen Coast, East Antarctica. Samples collected in the coastal areas showed higher concentrations of marine elements (Na, Ca, Mg, K, Li, and Sr), as well as Al, Fe, Mn, V, Cr, and Zn, compared to inland sites. In agreement with the above-mentioned studies, Zn, Cu, Mo, Cd, As, Se, Sb, and Pb were highly enriched compared to known natural sources, thus suggesting their anthropogenic origin. Calace et al. [49] investigated the presence of heavy metals (Cu, Zn, Cd, Pb, and As) associated with high-molecular-weight compounds in samples collected during the austral summer in 2005–2006 in Concordia Station (Dome C) along a trench having a 4 m depth. An increased metal concentration was obtained at a depth of 2.0–2.5 m, highlighting the formation of complexes between organic matter and heavy metals, thus resulting in the transportation of contaminants within the ice cores. Recently, Darham et al. published a review summarizing the occurrence of heavy metals in Antarctica and their remediation solutions [50]. The impacts of these compounds on the environment, ecosystems, and human health were also extensively described. It was observed that elements play a fundamental role in the biological processes of phytoplankton populations, impacting the whole marine ecosystem [51,52].

As for soot, it was detected in aerosols on Deception Island [53] and in surface snow collected from 28 sites across a transect of 2000 km from the northern tip of Antarctica to the southern Ellsworth Mountains [54]: concentrations in the 2–4 ng/g range were obtained in the areas surrounding research facilities and popular shore tourist-landing sites, whereas considerably lower amounts (~1 ng/g) were measured in remote areas. The major concern related to the presence of soot in snow is ascribed to the accelerated melting and shrinking processes of the Antarctic snowpack.

Concerning plastic particulate pollution, similar assumptions can be made. Even though Antarctica is considered uncontaminated land, the presence of micro- and nanoplastics has often been investigated in the last decade. Munari et al. [55] collected and analyzed by FT-IR several sediment samples from Terra Nova Bay during the 30th Antarctic Expedition in the austral summer of 2015. Various plastic particles with lengths in the 0.3–22 mm range made of nine different polymeric materials were detected. Fibers were the most frequent type of small plastic debris detected, with a decreasing concentration farther from the Mario Zucchelli research station. Reed et al. [56] analyzed sediments from intertidal and nearshore marine locations close to Rothera Research Station, Adelaide Island, in the west of the Antarctic Peninsula. Particles with characteristics similar to those commonly produced by clothes washing were recorded in sediment collected near the station sewage treatment plant outfall. In accordance with the above-mentioned findings, microplastic occurrence was also observed in Antarctic fish, as described by Zhu and coworkers [57]: polypropylene, polyamide, and polyethylene microparticles were present in fiber-like form in almost every investigated sample. The same polymers were the predominant plastics detected in sea ice samples collected by Kelly et al. [46] during the austral spring of 2009, 12 km north of Casey Station. An average concentration of 11 particles per liter was measured, highlighting the relationship between their occurrence and anthropogenic settlement. As for snow samples, using FT-IR, Aves et al. [37] analyzed samples collected from 19 sites in the Ross Island region. Microplastics, mostly polyethylene terephthalate in fiber form, were present in all snow samples at an average concentration of 29 particles per liter. Micro- and nanoplastic pollution in Antarctic snow was also deeply discussed by Citterich et al. in a recent review [58].

The common thread of these studies is the growing human footprint in Antarctica: the continuous and careful monitoring of snow, ice, seawater, and biota is of paramount importance for preserving such a delicate environment.

4. Conclusions

Although based on a reduced number of collected samples due to the pandemic event during the Antarctic campaign, this study confirms the pivotal role of Antarctica research in assessing the contributions and origins of small micro- and nanoparticles. In agreement with previous studies, micro- and nanoparticles related to anthropic activities were detected in snow samples collected in Terra Nova Bay, near active research stations. Considering that human activities in Antarctica are increasing, future expeditions should focus on the continuous monitoring of these materials in such remote areas to evaluate possible threats to the Antarctic environment and to better differentiate between local and long-range contamination so as to suggest actions for the preservation of the ecosystems.

The comparison of the results obtained by using different analytical techniques remains a challenging issue due to the scarcity of harmonized methods in monitoring studies. Technological developments in innovative complementary analytical approaches, including sample treatments and their standardization, represent major requirements to be faced in the near future for the development of an integrated approach encompassing all the relevant metrological tools. Only then will it be possible to define useful protocols for routine laboratories and the scientific community, allowing for the real advancement of research and the effective environmental management of micro- and nanopollutants. Another important key point to be addressed in the near future is the development of high-throughput nano-analytical systems able to simultaneously provide information about the morphology, amount, and chemical composition of the nanoparticles. To this aim, the separation of plastic and non-plastic materials will play a pivotal role.

Author Contributions: Conceptualization, F.B., N.R. and L.N.; methodology, F.B., N.R., L.N. and M.M. (Matteo Masino); formal analysis, F.B., N.R., L.N., M.M. (Matteo Masino) and M.M. (Monica Mattarozzi); investigation, L.N., M.M. (Matteo Masino), E.R. and M.P.; resources, F.B., L.N. and M.M. (Matteo Masino); writing—original draft preparation, F.B., N.R., L.N. and E.R.; writing—review and editing, all authors; visualization, F.B., L.N. and M.C.; supervision, F.B. and L.N.; project administration, F.B.; funding acquisition, F.B. All authors have read and agreed to the published version of the manuscript.

Funding: This study was supported by the project "Emerging Contaminants in Antarctic Snow: sources and TRAnsport (ECO AS:TRA)", funded by the MIUR Programma Nazionale di Ricerca in Antartide (PNRA), grant PNRA18_00229.

Institutional Review Board Statement: Not applicable.

Informed Consent Statement: Not applicable.

Data Availability Statement: The raw data supporting the conclusions of this article will be made available by the authors on request.

Acknowledgments: This work has benefited from the equipment and framework of the COMP-HUB and COMP-R Initiatives, funded by the "Departments of Excellence" program of the Italian Ministry for University and Research (MIUR, 2018–2022, and MUR, 2023–2027).

Conflicts of Interest: The authors declare no conflicts of interest.

References

1. Vecchiato, M.; Gambaro, A.; Kehrwald, N.M.; Ginot, P.; Kutuzov, S.; Mikhalenko, V.; Barbante, C. The Great Acceleration of Fragrances and PAHs Archived in an Ice Core from Elbrus, Caucasus. *Sci. Rep.* **2020**, *10*, 10661. [CrossRef] [PubMed]
2. D'Amico, M.; Gambaro, A.; Barbante, C.; Barbaro, E.; Caiazzo, L.; Vecchiato, M. Occurrence of the UV-Filter 2-Ethylhexyl 4-Methoxycinnimate (EHMC) in Antarctic Snow: First Results. *Microchem. J.* **2022**, *183*, 108060. [CrossRef]

3. Szopińska, M.; Potapowicz, J.; Jankowska, K.; Luczkiewicz, A.; Svahn, O.; Björklund, E.; Nannou, C.; Lambropoulou, D.; Polkowska, Ż. Pharmaceuticals and Other Contaminants of Emerging Concern in Admiralty Bay as a Result of Untreated Wastewater Discharge: Status and Possible Environmental Consequences. *Sci. Total Environ.* **2022**, *835*, 155400. [CrossRef] [PubMed]
4. Riboni, N.; Amorini, M.; Bianchi, F.; Pedrini, A.; Pinalli, R.; Dalcanale, E.; Careri, M. Ultra-Sensitive Solid-Phase Microextraction–Gas Chromatography–Mass Spectrometry Determination of Polycyclic Aromatic Hydrocarbons in Snow Samples Using a Deep Cavity BenzoQxCavitand. *Chemosphere* **2022**, *303*, 135144. [CrossRef]
5. Arcoleo, A.; Bianchi, F.; Careri, M. Helical Multi-Walled Carbon Nanotube-Coated Fibers for Solid-Phase Microextraction Determination of Polycyclic Aromatic Hydrocarbons at Ultra-Trace Levels in Ice and Snow Samples. *J. Chromatogr. A* **2020**, *1631*, 461589. [CrossRef]
6. Grotti, M.; Soggia, F.; Ardini, F.; Magi, E.; Becagli, S.; Traversi, R.; Udisti, R. Year-Round Record of Dissolved and Particulate Metals in Surface Snow at Dome Concordia (East Antarctica). *Chemosphere* **2015**, *138*, 916–923. [CrossRef]
7. Grotti, M.; Soggia, F.; Ardini, F.; Magi, E. Major and Trace Element Partitioning between Dissolved and Particulate Phases in Antarctic Surface Snow. *J. Environ. Monit.* **2011**, *13*, 2511–2520. [CrossRef]
8. Mattarozzi, M.; Bianchi, F.; Maffini, M.; Vescovi, F.; Catellani, D.; Suman, M.; Careri, M. ESEM-EDS-Based Analytical Approach to Assess Nanoparticles for Food Safety and Environmental Control. *Talanta* **2019**, *196*, 429–435. [CrossRef]
9. Llorca, M.; Farré, M. Micromaterials and Nanomaterials as Potential Emerging Pollutants in the Marine Environment. In *Contaminants of Emerging Concern in the Marine Environment*; Elsevier: Amsterdam, The Netherlands, 2023; pp. 375–400.
10. Waller, C.L.; Griffiths, H.J.; Waluda, C.M.; Thorpe, S.E.; Loaiza, I.; Moreno, B.; Pacherres, C.O.; Hughes, K.A. Microplastics in the Antarctic Marine System: An Emerging Area of Research. *Sci. Total Environ.* **2017**, *598*, 220–227. [CrossRef]
11. Materić, D.; Kjær, H.A.; Vallelonga, P.; Tison, J.L.; Röckmann, T.; Holzinger, R. Nanoplastics Measurements in Northern and Southern Polar Ice. *Environ. Res.* **2022**, *208*, 112741. [CrossRef] [PubMed]
12. Rodríguez-Félix, F.; Graciano-Verdugo, A.Z.; Moreno-Vásquez, M.J.; Lagarda-Díaz, I.; Barreras-Urbina, C.G.; Armenta-Villegas, L.; Olguín-Moreno, A.; Tapia-Hernández, J.A. Trends in Sustainable Green Synthesis of Silver Nanoparticles Using Agri-Food Waste Extracts and Their Applications in Health. *J. Nanomater.* **2022**, *2022*, 8874003. [CrossRef]
13. Tran, T.K.; Nguyen, M.K.; Lin, C.; Hoang, T.D.; Nguyen, T.C.; Lone, A.M.; Khedulkar, A.P.; Gaballah, M.S.; Singh, J.; Chung, W.J.; et al. Review on Fate, Transport, Toxicity and Health Risk of Nanoparticles in Natural Ecosystems: Emerging Challenges in the Modern Age and Solutions toward a Sustainable Environment. *Sci. Total Environ.* **2024**, *912*, 169331. [CrossRef] [PubMed]
14. Dobrică, E.; Engrand, C.; Leroux, H.; Rouzaud, J.N.; Duprat, J. Transmission Electron Microscopy of CONCORDIA Ultracarbonaceous Antarctic Micrometeorites (UCAMMS): Mineralogical Properties. *Geochim. Cosmochim. Acta* **2012**, *76*, 68–82. [CrossRef]
15. Esquivel, E.; Murr, L. A TEM Analysis of Nanoparticulates in a Polar Ice Core. *Mater. Charact.* **2004**, *52*, 15–25. [CrossRef]
16. Weinbruch, S.; Zou, L.; Ebert, M.; Benker, N.; Drotikova, T.; Kallenborn, R. Emission of Nanoparticles from Coal and Diesel Fired Power Plants on Svalbard: An Electron Microscopy Study. *Atmos. Environ.* **2022**, *282*, 119138. [CrossRef]
17. Beltrami, D.; Calestani, D.; Maffini, M.; Suman, M.; Melegari, B.; Zappettini, A.; Zanotti, L.; Casellato, U.; Careri, M.; Mangia, A. Development of a Combined SEM and ICP-MS Approach for the Qualitative and Quantitative Analyses of Metal Microparticles and Sub-Microparticles in Food Products. *Anal. Bioanal. Chem.* **2011**, *401*, 1401–1409. [CrossRef] [PubMed]
18. Ghosh, S.; Di, Z.; Pan, B.; Xing, B. Application of Atomic Force Microscopy (AFM) on Environmental Interfaces. In *Encyclopedia of Soils in the Environment*; Elsevier: Amsterdam, The Netherlands, 2023; pp. 589–604.
19. Meyer, E.; Pawlak, R.; Glatzel, T. Scanning Probe Microscopy. In *Encyclopedia of Condensed Matter Physics*; Elsevier: Amsterdam, The Netherlands, 2024; pp. 51–62.
20. Ren, Y.; Zhang, X.; Wei, H.; Xu, L.; Zhang, J.; Sun, J.; Wang, X.; Li, W. Comparisons of Methods to Obtain Insoluble Particles in Snow for Transmission Electron Microscopy. *Atmos. Environ.* **2017**, *153*, 61–69. [CrossRef]
21. Ellis, A.; Edwards, R.; Saunders, M.; Chakrabarty, R.K.; Subramanian, R.; Van Riessen, A.; Smith, A.M.; Lambrinidis, D.; Nunes, L.J.; Vallelonga, P.; et al. Characterizing Black Carbon in Rain and Ice Cores Using Coupled Tangential Flow Filtration and Transmission Electron Microscopy. *Atmos. Meas. Tech.* **2015**, *8*, 3959–3969. [CrossRef]
22. Cai, H.; Xu, E.G.; Du, F.; Li, R.; Liu, J.; Shi, H. Analysis of Environmental Nanoplastics: Progress and Challenges. *Chem. Eng. J.* **2021**, *410*, 128208. [CrossRef]
23. Okoffo, E.D.; Thomas, K.V. Quantitative Analysis of Nanoplastics in Environmental and Potable Waters by Pyrolysis-Gas Chromatography–Mass Spectrometry. *J. Hazard. Mater.* **2024**, *464*, 133013. [CrossRef]
24. Chen, Q.; Wang, J.; Yao, F.; Zhang, W.; Qi, X.; Gao, X.; Liu, Y.; Wang, J.; Zou, M.; Liang, P. A Review of Recent Progress in the Application of Raman Spectroscopy and SERS Detection of Microplastics and Derivatives. *Microchim. Acta* **2023**, *190*, 465. [CrossRef] [PubMed]
25. Bianchi, F.; Riboni, N.; Trolla, V.; Furlan, G.; Avantaggiato, G.; Iacobellis, G.; Careri, M. Differentiation of Aged Fibers by Raman Spectroscopy and Multivariate Data Analysis. *Talanta* **2016**, *154*, 467–473. [CrossRef]
26. Li, Y.; Wu, M.; Li, H.; Xue, H.; Tao, J.; Li, M.; Wang, F.; Li, Y.; Wang, J.; Li, S. Current Advances in Microplastic Contamination in Aquatic Sediment: Analytical Methods, Global Occurrence, and Effects on Elemental Cycling. *TrAC Trends Anal. Chem.* **2023**, *168*, 117331. [CrossRef]

27. Cincinelli, A.; Scopetani, C.; Chelazzi, D.; Lombardini, E.; Martellini, T.; Katsoyiannis, A.; Fossi, M.C.; Corsolini, S. Microplastic in the Surface Waters of the Ross Sea (Antarctica): Occurrence, Distribution and Characterization by FTIR. *Chemosphere* **2017**, *175*, 391–400. [CrossRef] [PubMed]
28. Eom, H.-J.; Gupta, D.; Cho, H.-R.; Hwang, H.J.; Hur, S.D.; Gim, Y.; Ro, C.-U. Single-Particle Investigation of Summertime and Wintertime Antarctic Sea Spray Aerosols Using Low-*Z* Particle EPMA, Raman Microspectrometry, and ATR-FTIR Imaging Techniques. *Atmos. Chem. Phys.* **2016**, *16*, 13823–13836. [CrossRef]
29. Materić, D.; Kasper-Giebl, A.; Kau, D.; Anten, M.; Greilinger, M.; Ludewig, E.; Van Sebille, E.; Röckmann, T.; Holzinger, R. Micro-and Nanoplastics in Alpine Snow: A New Method for Chemical Identification and (Semi)Quantification in the Nanogram Range. *Environ. Sci. Technol.* **2020**, *54*, 2353–2359. [CrossRef] [PubMed]
30. Stefánsson, H.; Peternell, M.; Konrad-Schmolke, M.; Hannesdóttir, H.; Ásbjörnsson, E.J.; Sturkell, E. Microplastics in Glaciers: First Results from the Vatnajökull Ice Cap. *Sustainability* **2021**, *13*, 4183. [CrossRef]
31. Mariano, S.; Tacconi, S.; Fidaleo, M.; Rossi, M.; Dini, L. Micro and Nanoplastics Identification: Classic Methods and Innovative Detection Techniques. *Front. Toxicol.* **2021**, *3*, 636640. [CrossRef]
32. Petrucci, R.; Chiarotto, I.; Mattiello, L.; Pandolfi, F.; Rocco, D.; Zollo, G.; Feroci, M. High Performance Liquid Chromatography Coupled with Mass Spectrometry for/and Nanomaterials: An Overview. In *AIP Conference Proceedings*; AIP: Melville, NY, USA, 2020; p. 020002.
33. Mattarozzi, M.; Careri, M. Liquid Chromatography/Mass Spectrometry in Environmental Analysis. In *Encyclopedia of Analytical Chemistry*; Wiley: Hoboken, NJ, USA, 2023; pp. 1–30.
34. Becagli, S.; Barbaro, E.; Bonamano, S.; Caiazzo, L.; Di Sarra, A.; Feltracco, M.; Grigioni, P.; Heintzenberg, J.; Lazzara, L.; Legrand, M.; et al. Factors Controlling Atmospheric DMS and Its Oxidation Products (MSA and $NssSO_4^{2-}$) in the Aerosol at Terra Nova Bay, Antarctica. *Atmos. Chem. Phys.* **2022**, *22*, 9245–9263. [CrossRef]
35. Feltracco, M.; Zangrando, R.; Barbaro, E.; Becagli, S.; Park, K.T.; Vecchiato, M.; Caiazzo, L.; Traversi, R.; Severi, M.; Barbante, C.; et al. Characterization of Free L- and D-Amino Acids in Size-Segregated Background Aerosols over the Ross Sea, Antarctica. *Sci. Total Environ.* **2023**, *879*, 163070. [CrossRef] [PubMed]
36. Thamban, M.; Thakur, R.C. Trace Metal Concentrations of Surface Snow from Ingrid Christensen Coast, East Antarctica—Spatial Variability and Possible Anthropogenic Contributions. *Environ. Monit. Assess.* **2013**, *185*, 2961–2975. [CrossRef] [PubMed]
37. Aves, A.R.; Revell, L.E.; Gaw, S.; Ruffell, H.; Schuddeboom, A.; Wotherspoon, N.E.; Larue, M.; Mcdonald, A.J. First Evidence of Microplastics in Antarctic Snow. *Cryosphere* **2022**, *16*, 2127–2145. [CrossRef]
38. Balakrishna, K.; Praveenkumarreddy, Y.; Nishitha, D.S.; Gopal, C.M.; Shenoy, J.K.; Bhat, K.; Khare, N.; Dhangar, K.; Kumar, M. Occurrences of UV Filters, Endocrine Disruptive Chemicals, Alkyl Phenolic Compounds, Fragrances, and Hormones in the Wastewater and Coastal Waters of the Antarctica. *Environ. Res.* **2023**, *222*, 115327. [CrossRef]
39. Sze, S.-K.; Siddique, N.; Sloan, J.J.; Escribano, R. Raman Spectroscopic Characterization of Carbonaceous Aerosols. *Atmos. Environ.* **2001**, *35*, 561–568. [CrossRef]
40. Ferrugiari, A.; Tommasini, M.; Zerbi, G. Raman Spectroscopy of Carbonaceous Particles of Environmental Interest. *J. Raman Spectrosc.* **2015**, *46*, 1215–1224. [CrossRef]
41. Feng, Y.; Liu, L.; Yang, Y.; Deng, Y.; Li, K.; Cheng, H.; Dong, X.; Li, W.; Zhang, L. The application of Raman spectroscopy combined with multivariable analysis on source apportionment of atmospheric black carbon aerosols. *Sci. Total Environ.* **2019**, *685*, 189–196. [CrossRef] [PubMed]
42. Andrés López Ray, L.; Frost, Y.X.; Scholz, R. Vibrational Spectroscopic Characterization of the Sulphate-Carbonate Mineral Burkeite: Implications for Evaporites. *Spectrosc. Lett.* **2014**, *47*, 564–570. [CrossRef]
43. Frezzotti, M.L.; Tecce, F.; Casagli, A. Raman Spectroscopy for Fluid Inclusion Analysis. *J. Geochemical Explor.* **2012**, *112*, 1–20. [CrossRef]
44. Andrés López Ray, L.; Frost, Y.X.; Scholz, R. A Vibrational Spectroscopic Study of the Sulfate Mineral Glauberite. *Spectrosc. Lett.* **2014**, *47*, 740–745. [CrossRef]
45. Bao, H.; Campbell, D.A.; Bockheim, J.G.; Thiemens, M.H. Origins of Sulphate in Antarctic Dry-Valley Soils as Deduced from Anomalous 17O Compositions. *Nature* **2000**, *407*, 499–502. [CrossRef]
46. Kelly, A.; Lannuzel, D.; Rodemann, T.; Meiners, K.M.; Auman, H.J. Microplastic Contamination in East Antarctic Sea Ice. *Mar. Pollut. Bull.* **2020**, *154*, 111130. [CrossRef]
47. Desai, U.; Sharma, B.K.; Singh, A.; Singh, A. Enhancement of Resistance against Damp Heat Aging through Compositional Change in PV Encapsulant Poly (Ethylene-Co-Vinyl Acetate). *Sol. Energy* **2020**, *211*, 674–682. [CrossRef]
48. Bazzano, A.; Soggia, F.; Grotti, M. Source Identification of Atmospheric Particle-Bound Metals at Terra Nova Bay, Antarctica. *Environ. Chem.* **2015**, *12*, 245–252. [CrossRef]
49. Calace, N.; Nardi, E.; Pietroletti, M.; Bartolucci, E.; Pietrantonio, M.; Cremisini, C. Antarctic Snow: Metals Bound to High Molecular Weight Dissolved Organic Matter. *Chemosphere* **2017**, *175*, 307–314. [CrossRef]
50. Darham, S.; Zakaria, N.N.; Zulkharnain, A.; Sabri, S.; Khalil, K.A.; Merican, F.; Gomez-Fuentes, C.; Lim, S.; Ahmad, S.A. Antarctic Heavy Metal Pollution and Remediation Efforts: State of the Art of Research and Scientific Publications. *Braz. J. Microbiol.* **2023**, *54*, 2011–2026. [CrossRef]

51. Gerringa, L.J.A.; Alderkamp, A.C.; Laan, P.; Thuróczy, C.E.; De Baar, H.J.W.; Mills, M.M.; van Dijken, G.L.; Haren, H.; van Arrigo, K.R. Iron from Melting Glaciers Fuels the Phytoplankton Blooms in Amundsen Sea (Southern Ocean): Iron Biogeochemistry. *Deep. Res. Part II Top. Stud. Oceanogr.* **2012**, *71*, 16–31. [CrossRef]
52. Tian, H.A.; van Manen, M.; Wille, F.; Jung, J.; Lee, S.H.; Kim, T.W.; Aoki, S.; Eich, C.; Brussaard, C.P.D.; Reichart, G.J.; et al. The Biogeochemistry of Zinc and Cadmium in the Amundsen Sea, Coastal Antarctica. *Mar. Chem.* **2023**, *249*, 104223. [CrossRef]
53. Marina-Montes, C.; Pérez-Arribas, L.V.; Anzano, J.; de Vallejuelo, S.F.-O.; Aramendia, J.; Gómez-Nubla, L.; de Diego, A.; Manuel Madariaga, J.; Cáceres, J.O. Characterization of Atmospheric Aerosols in the Antarctic Region Using Raman Spectroscopy and Scanning Electron Microscopy. *Spectrochim. Acta Part A Mol. Biomol. Spectrosc.* **2022**, *266*, 120452. [CrossRef] [PubMed]
54. Cordero, R.R.; Sepúlveda, E.; Feron, S.; Damiani, A.; Fernandoy, F.; Neshyba, S.; Rowe, P.M.; Asencio, V.; Carrasco, J.; Alfonso, J.A.; et al. Black Carbon Footprint of Human Presence in Antarctica. *Nat. Commun.* **2022**, *13*, 984. [CrossRef] [PubMed]
55. Munari, C.; Infantini, V.; Scoponi, M.; Rastelli, E.; Corinaldesi, C.; Mistri, M. Microplastics in the Sediments of Terra Nova Bay (Ross Sea, Antarctica). *Mar. Pollut. Bull.* **2017**, *122*, 161–165. [CrossRef] [PubMed]
56. Reed, S.; Clark, M.; Thompson, R.; Hughes, K.A. Microplastics in Marine Sediments near Rothera Research Station, Antarctica. *Mar. Pollut. Bull.* **2018**, *133*, 460–463. [CrossRef] [PubMed]
57. Zhu, W.; Zhao, N.; Liu, W.; Guo, R.; Jin, H. Occurrence of Microplastics in Antarctic Fishes: Abundance, Size, Shape, and Polymer Composition. *Sci. Total Environ.* **2023**, *903*, 166186. [CrossRef] [PubMed]
58. Citterich, F.; Lo Giudice, A.; Azzaro, M. A Plastic World: A Review of Microplastic Pollution in the Freshwaters of the Earth's Poles. *Sci. Total Environ.* **2023**, *869*, 161847. [CrossRef] [PubMed]